

J3J.4 THE DIURNAL CYCLE OF RAINFALL AND THE IDENTIFICATION OF RAINFALL REGIMES WITHIN THE NORTH AMERICAN MONSOON OF NW MEXICO

D. A. Ahijevych*, R. E. CARBONE, T. J. LANG¹, AND A. V.-MANZANILLA²

*National Center for Atmospheric Research, Boulder, Colorado

¹Colorado State University, Fort Collins, CO

²Juarez University, Tobasco, Mexico

1 INTRODUCTION

During the summer of 2004, a special observing network, including three ground-based Doppler radars, monitored a region of northwest Mexico. As part of the North American Monsoon Experiment (NAME), these radars surveyed precipitation and wind for a six week period following monsoon onset in the region northwest of Mazatlan. This region is known to have complex interactions among easterly waves, tropical cyclones, and deep convection over the Sierra Madre Occidental (SMO) and the Gulf of California (GoC). The radars performed rainfall climatology scans at 15 minute intervals nearly 24 hours per day for the period of record. We present preliminary findings on the diurnal cycle of rainfall and the variability observed in regimes of convection. We further stratify the diurnal cycle data for both regimes.

2 METHODOLOGY

Our approach follows the reduced-dimension analysis methods of Carbone et al (2002). We examine the onset and movement of convection both parallel and perpendicular to the SMO and the GoC coastline, assuming that thermal forcing strongly influences the observed rainfall patterns. Fig. 1 shows the region covered by the radar network after rotating the domain such that the SMO and GoC are aligned with the y-axis.

For the composites, where radar lobes intersect, we use the gates closest to the surface and have removed ground clutter, fixed beam blockage, and subtracted reflectivity biases between S-Pol and the other two SMN radars. Using polarimetric variables such as specific differential phase shift (K_{dp}) and differential reflectivity (Z_{dr}), we produced refined rainfall maps in the Spol coverage region and developed appropriate reflectivity-rainrate (Z-R) relationships for the adjacent SMN radars.

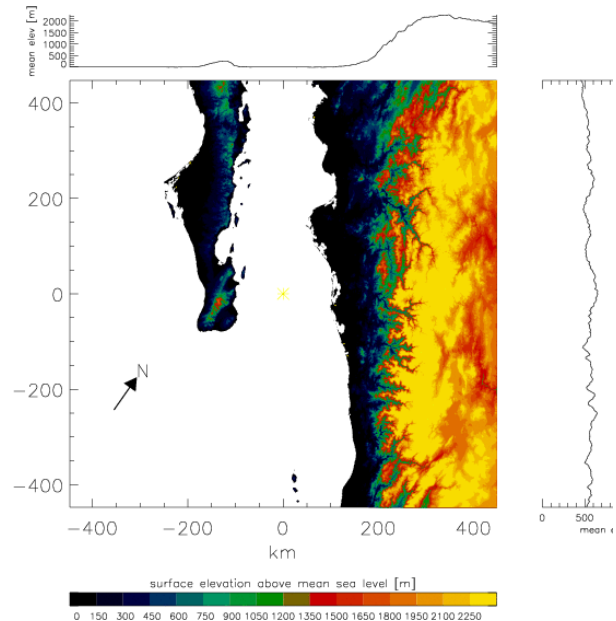


Fig. 1. The radar network domain was rotated 35 deg clockwise to align topography with the y-axis. True north is indicated by the black arrow. Terrain elevation is shaded and the mean elevation profiles are graphed above and to the right of the plan view.

The averaging domain used for the Hovmöller diagrams is encompassed by the black box in Fig. 2. This domain is close to the radars where the beam is near the surface and avoids areas with frequently missing data since a small number of samples may bias the results. At least 100 valid non-missing data points were required when averaging each row or column. Data points were on a ~2 km grid.

*Corresponding author address: David Ahijevych,
NCAR, P.O Box 3000 Boulder, CO 80307, e-mail:
ahijevyc@ucar.edu

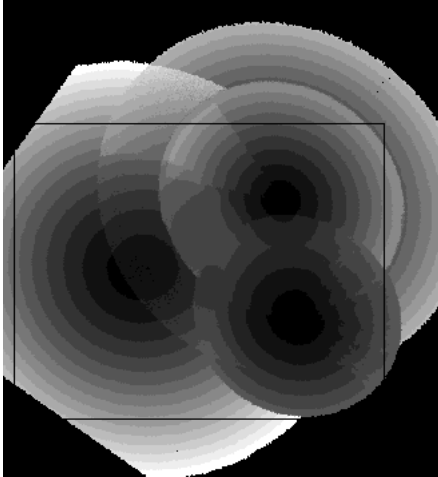


Fig. 2. Grey circles show coverage of the 3-radar network over the same domain as in Fig. 1. The black rectangle outlines the sub-domain of the Hovmöller diagrams. Shading is height of the radar beam and ranges from 0 (black) to 15 km (white).

3 RESULTS

We observe at least two regimes:

1. A diurnally-forced "undisturbed" regime in which rainfall originates over high terrain of the SMO and subsequently moves westward to the coast during the late afternoon, and
2. A "disturbed" regime (or regimes), which exhibits considerable variability with respect to diurnal forcing.

The "undisturbed" regime: mainly produces rainfall in the region between the upper SMO and the mid-GoC; is heavily influenced by the elevated heat source and breeze circulations; and exhibits relatively little propagation of organized convection parallel to the mountains and the coast. This is summarized in Fig. 3. The reflectivity averaged perpendicular to the coast and parallel to the coast show most of the diurnal variability of precipitation is in the cross-coast dimension (left half of figure). The greatest values occur over land from 1400-2300 local time (local time = UTC-6h) and move left, toward the GoC, at night. The secondary maximum on the left of the figure is just west of the Baja peninsula.

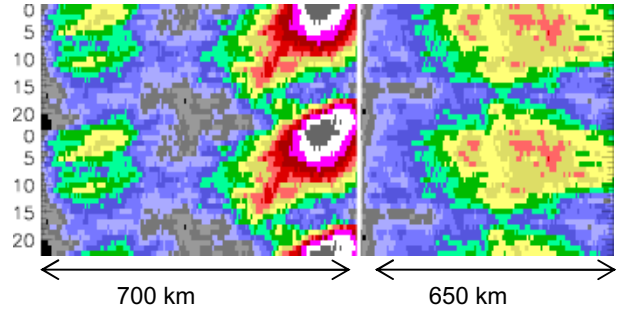


Fig. 3. Cross-coast-average reflectivity (left) and along-coast-average reflectivity (right) by diurnal hour (y-axis in UTC). In this figure, reflectivity has been normalized, so no scale is available, and the diurnal cycle has been repeated for clarity.

The "disturbed" regime is often associated with longer-lived precipitation episodes and/or northward propagation nearly parallel to the coast. At least some of these events are associated with one or more of the following: so-called Gulf "surges" of southerly momentum; the passage of easterly waves; and the movement of tropical cyclones, which are often located to the south of our domain. See Fig. 4 for the corresponding diurnal cycle of the disturbed regime. The main precipitation peak that initiates over land extends further left into the GoC and lasts longer than in the "undisturbed" regime. This seaward translation speed is about 5 m/s. There is also the possibility of coherent propagation in the along-coast dimension (right part of Fig. 4) as suggested by the downward streaks.

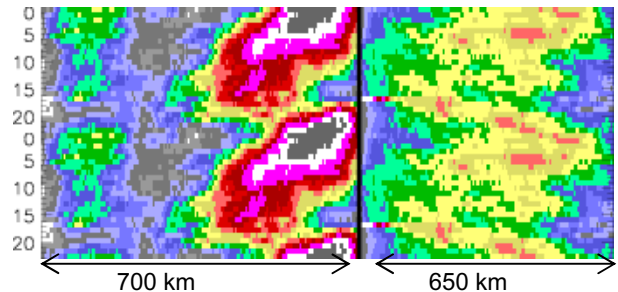
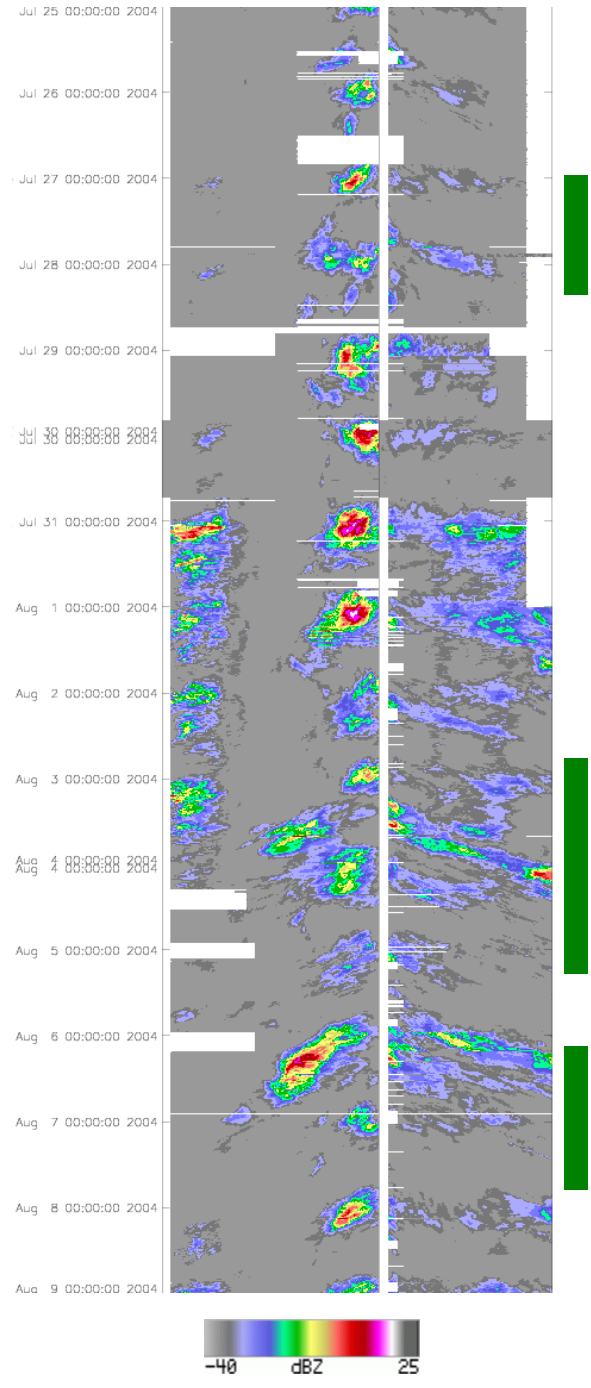
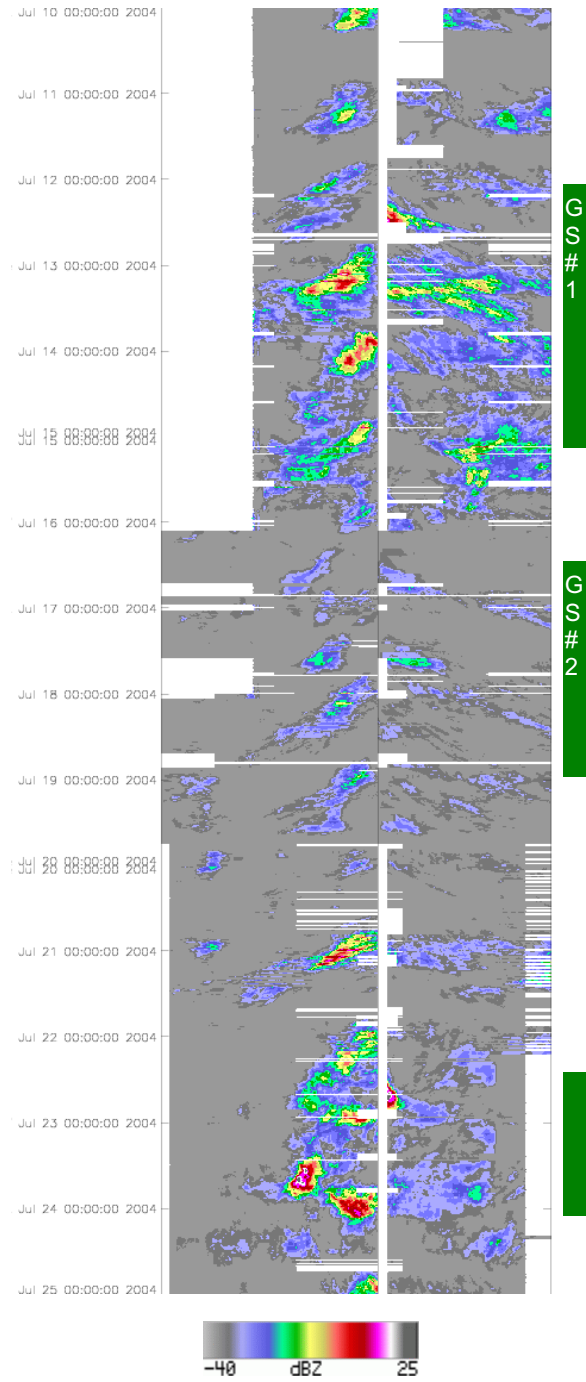


Fig. 4. Diurnal cycle of reflectivity as in Fig. 2 except for "disturbed" regime.

4 DISCUSSION

We have examined the diurnal cycle and its variability to quantify the wind and rainfall patterns observed during NAME. These mesoscale observations should help to define the most important processes in regional climate circulations and ultimately improve the representation of convective rainfall in climate system models. Hovmöller diagrams help to elucidate certain regime changes such as easterly waves, monsoon break periods, and Gulf surges, in addition to highlighting long-lived precipitation episodes in the region. The statistics should help to define controlling factors in the regional climatology of rainfall and lead to

improvements in the representation of convection for regional climate and NWP models.



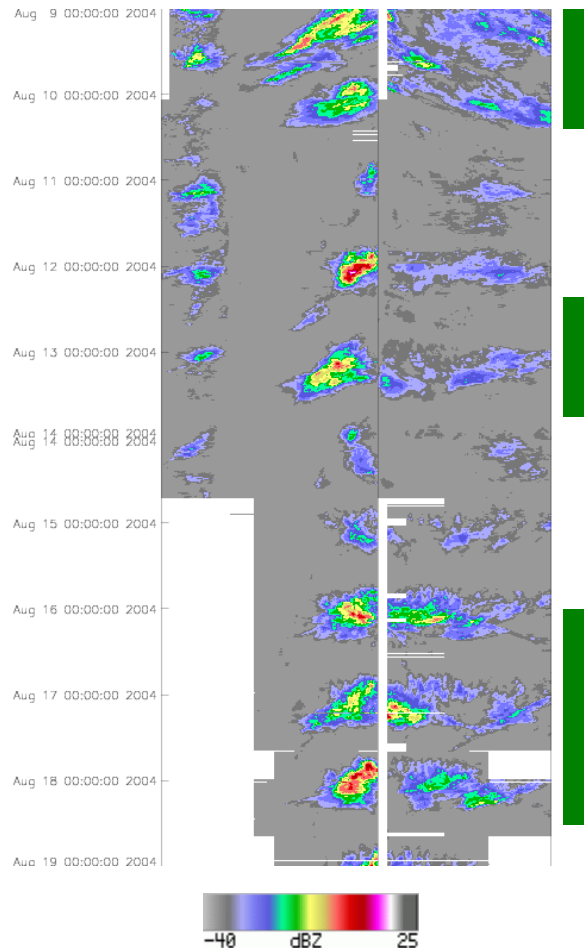


Fig. 5. 40-day Hovmöller diagrams of average reflectivity. Domain is shown in Figs. 1 and 2. Time (UTC) increases downward. For the left part, the x-axis is normal to the coastline (i.e. Baja peninsula and ocean on the left; Mexican mainland on the right) and for the right part, the x-axis is parallel to the coastline (northward is to the right). Regime changes associated with Gulf Surges (GS #1, GS #2) are readily apparent as extensions of rainfall activity into the coastal waters during the night. Disturbed regimes are highlighted with a colored bar on the right side of the figure. During these periods, northward-propagating systems are often evident (in the right part of the figure).

5 REFERENCES

Carbone, R. E., J. D. Tuttle, D. A. Ahijevych, and S. B. Trier, 2002: Inferences of predictability associated with warm season precipitation episodes. *J. Atmos. Sci.*, 59 (13), 2033-2056.